

## Polymeric optical fibre sensor coated by SiO<sub>2</sub> nanoparticles for humidity sensing in the skin microenvironment

David Gomez, Stephen P. Morgan, Barrie R. Hayes-Gill, Ricardo Goncalves Correia, Sergiy Korposh

Optics and Photonics Research Group, Faculty of Engineering, University Park, University of Nottingham, Nottingham, NG7 2RD, UK

Corresponding author: Sergiy Korposh, [s.korposh@nottingham.ac.uk](mailto:s.korposh@nottingham.ac.uk)

### ABSTRACT

The sensitivity of a low-cost polymeric optical fibre humidity sensor based on transmittance changes due to evanescent wave absorption is reported using test measurements in an environmental chamber and of the skin. The layer-by-layer method was used to coat 30mm of the central unclad section of a multimode polymeric optical fibre with 7 layers of a hydrophilic film consisting of bilayers of poly(allylamine hydrochloride) and SiO<sub>2</sub> mesoporous nanoparticles. Sensor characterisation shows a decrease in light transmission as relative humidity increases as a result of refractive index changes of the coating deposited onto the optical fibre which correlates with a commercial capacitive humidity sensor. The sensitivity obtained for the sensor coated with an optimum 7 layers was approximately  $-3.87 \times 10^{-3}$  and  $-9.61 \times 10^{-3}$  in transmittance percentage per RH percentage for the range of ~10% to ~75% RH and 90% to 97% RH, respectively. In addition, a response time of 1.5s can be seen for breath monitoring with the polymeric optical fibre humidity sensor. The proof of concept measurements made on the skin indicate that this sensor has the potential to be used to monitor humidity of the skin microenvironment within a wound dressing which can be used to provide better prognosis of healing.

**Keywords:** Polymeric optical fibre humidity sensor, evanescent wave, layer-by-layer, hydrophilic film, relative humidity.

## 1. Introduction

Humidity measurements are important for several aspects of daily life, such as air conditioning, meteorological forecast and in industrial settings. Furthermore, there are medical conditions that would benefit from humidity monitoring, such as monitoring of air delivered to mechanically ventilated patients in critical care [1] and monitoring the microenvironment of chronic wounds [2]. Chronic wounds are a major global healthcare problem placing a considerable economic burden on the resources of healthcare providers. For example, in the UK alone, a recent analysis of the health economic burden of wounds [3] highlighted that ~2.2 million wounds were managed by the publicly funded National Health Service (NHS) in 2012/2013 requiring 18.6 million practice nurse, 10.9 million community nurse, 7.7 million GP and 3.4 million hospital outpatient visits. The annual NHS cost of managing these wounds is £4.5-5.1 billion (~4% of the entire NHS budget). A wound dressing that remotely monitors parameters associated with healing such as humidity presented on the wound microenvironment, wound exudate pH and proliferative cell levels within the wound could have a significant impact on these costs. This monitoring would enable clinical interventions to take place promptly but only when required, thus improving wound care and reducing the number of clinical appointments.

Studies by Winter [2] have demonstrated the advantages of keeping a moist environment at the wound surface rather than allowing the wound to dry out. It has been shown that the healing rate is at least twice faster when the wound is covered by a dressing in order to maintain optimal hydration [4]. Moisture on wounds accelerates the epithelialization phase of wound healing by preventing scab formation over the wound bed. This increases migration of proliferative cells, such as fibroblast and endothelial cells that produces angiogenesis and promotes growth factors and keratinocytes, which results in faster dermal repair and reduced scarring of the wound [5] [6] [7]. Additionally, it has been shown that moist wounds decrease bacterial infection by the formation of a hostile antibacterial environment [8]. However an equilibrium in humidity should be reached in order to avoid skin breakdown and delayed healing [9] [10].

In order to preserve a moist environment on the wound surface, humidity can be measured. The level of humidity is quantified by the term relative humidity (RH), which is defined as the ratio of water vapour present in the environment to the maximum amount of water that the

environment can hold, expressed as a percentage. Several devices exist to measure humidity [11]; many of them are either expensive or not suitable to be embedded within wound dressings. Previous research has incorporated electrochemical sensors into wound dressings [12] [13] [14] but optical fibre sensors (OFS) have not yet been investigated in such a setting. These potentially offer a more convenient and reliable alternative method of monitoring humidity [15] [16] as they have low-cost fabrication, small size and diameter (micrometres), fast response and high sensitivity [17].

Previous research has shown different approaches of humidity sensors based on silica core fibre [1] [18] [19]. However, it is known that a silica core fibre may not be suitable for use in a harsh environment due to its fragility after removing the cladding. In contrast, polymeric optical fibres (POF) have higher elasticity and strength to resist rough handling that makes them well suited to be embedded within wound dressings [20]. In the work presented in this paper, the fabrication and characterisation of a polymeric optical fibre humidity sensor (POFHS) is described. The unclad central region of the POF was coated by a hydrophilic mesoporous film based on poly(allylamine hydrochloride) (PAH) and SiO<sub>2</sub> mesoporous nanoparticles (PAH/SiO<sub>2</sub>) using a layer-by-layer (LbL) deposition method [21]. The principle of operation of the POFHS is based on the measurements of the light intensity changes due to the interaction between the evanescent wave (EW) and the hydrophilic film, which changes its refractive index with humidity.

The ultimate objective of this work is to develop an optical fibre sensor that can be embedded into a textile, such as wound dressings in order to provide humidity measurements of the wound microenvironment without removing the dressing and hence disturbing the wound healing process. Our work aims to provide a better prognosis of wound healing that can result in a reduction of hospitalization time, prevention of advanced treatments such as surgery, reduced referrals and hence reduced health care costs [22]. The ability to predict the efficiency of wound healing will help ensure patients receive the appropriate attention at the earliest possible stage. In this work, as an initial step, the fibre was embedded into a textile and humidity generated from the intact skin was measured to prove the concept. An example is also provided within a wound dressing.

## 2. Material and Methods

This section describes the sensor fabrication and monitoring process and two experiments that were carried out to demonstrate the sensitivity of the POFHS as a function of humidity: the first in an environment where humidity was controlled by flowing nitrogen through a gas chamber and another using humidity generated from the palm of a hand.

### 2.1 *Sensor fabrication*

ESKA SK-10 multimode POF (1.49 refractive index, 0.5 NA, Mitsubishi Rayon Co., Ltd.) with the core diameter of 240 $\mu$ m polymethyl-methacrylate resin (PMMA) and 5 $\mu$ m fluorinated polymer cladding was used. In order to facilitate interaction between the mesoporous thin film and EW the cladding was removed to expose the core in a region around the mid-section of the fibre. The optical fibre was placed within a holder made of Teflon containing a channel of dimensions 50mm length, 5mm width and 7mm height and exposed to acetone ( $(\text{CH}_3)_2\text{CO}$ ) in order to remove the cladding. The diameter of the optical fibre after cladding removal was measured using a microscope (BX50F4, Olympus optical Co. Ltd.).

Since the POF cladding is only 5 $\mu$ m thick, it can be easily removed. Nonetheless, it was observed that by removing also a small part of the core, a more uniform surface is achieved in order to obtain better film deposition and hence higher sensitivity due to enhanced interaction between EW and the humidity sensitive film. Scanning electron microscopy (SEM) (Philips (FEI) XL30 FEG ESEM) images from the unclad section of the fibre were taken in order to observe uniformity of the unclad surface of the fibre. For SEM measurements the unclad section of the fibre was coated with platinum (Pt) using sputtering coating method.

Once the cladding and a part of the core are removed the humidity sensitive film is deposited using the LbL method. SiO<sub>2</sub> mesoporous nanoparticles (SNOWTEX 20L, 40-50nm diameter, Nissan Chemical, Japan) were deposited with poly(allylamine hydrochloride) (PAH) to form a PAH/SiO<sub>2</sub> hydrophilic material which creates a higher humidity sensitivity compared with microporous and macroporous materials [23].

The PAH/SiO<sub>2</sub> layers were deposited in three steps as illustrated in Figure 1 [24]. First, the unclad surface of the POF is placed within the Teflon holder. The core surface is activated by depositing 1wt% ethanolic KOH in order to functionalise it with OH<sup>-</sup> groups. After 20 min, KOH is removed using an aspiration pump and the fibre is rinsed and dried with deionized water and Nitrogen gas (N<sub>2</sub>), respectively.

Second, the fibre is bathed with 0.17wt% of positively charged PAH (Sigma-Aldrich Co, UK, polycation, pH = 11) for 15 min. After the polycation deposition, the fibre is washed and dried again. The third stage is to immerse the fibre in a solution containing negatively charged SiO<sub>2</sub> nanoparticles for 15 min. Then the fibre is once again washed and dried in order to remove any excess nanoparticles and obtain a uniform monolayer. In order to deposit more layers, the second and the third steps are repeated.

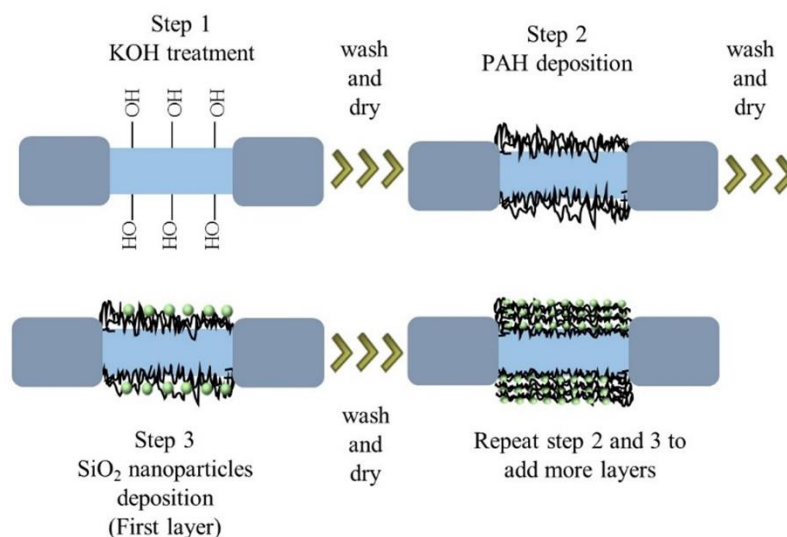


**Figure 1.** Layer-by-Layer deposition process.

The cladding removal and LbL deposition processes were monitored using the set-up illustrated in Figure 2. It consists of a tungsten halogen lamp (Ocean Optics HL-2000, wavelength range  $\lambda = 360\text{nm} - 2400\text{nm}$ ) connected to one end of a POF via an SMA connector. At the other end of the fibre, intensity light changes produced by the interaction of the humidity sensor with the surrounding environment were monitored by a spectrometer (Ocean Optics USB 2000+, detection range  $\lambda = 200\text{nm} - 1100\text{nm}$ ). The spectrometer is connected to a computer via a USB port in order to control the spectrometer and record the data.

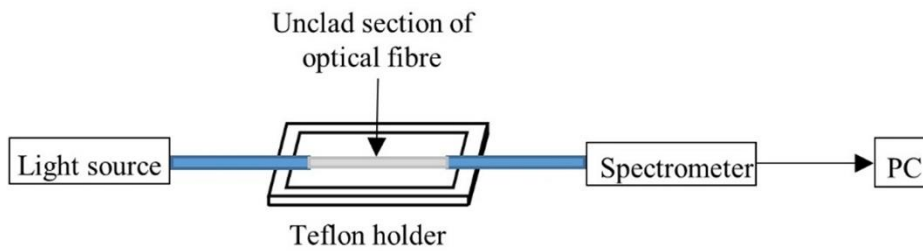


**Figure 2.** Set-up for monitoring POFHS fabrication process.

## 2.2 *In-vitro* humidity measurement using flowmeter setup

The in-vitro experimental set-up for generating humidity of different levels is illustrated in Figure 3. Nitrogen gas is supplied to two flowmeters,  $F_1$  and  $F_2$  (range 0.1 – 1 L/min, Cole-Parmer Instrument Co. Ltd.).  $F_1$  supplies nitrogen gas directly to one input of a plastic three-way stopcock valve whilst  $F_2$  is connected to a heated flask filled with water. Once evaporation of water begins, vapour is transported from the flask to the other input of the stopcock valve in order to mix flows from  $F_1$  (direct  $N_2$  low humidity) and  $F_2$  (water vapour, high humidity). The combination of  $F_1$  and  $F_2$  provides different levels of RH. The inflow from the stopcock valve output was connected to the lid of a Petri dish via a pipe. Plastic paraffin film was used to seal the pipe with the lid and the rest of the Petri dish in order to avoid leakage.

To generate different levels of humidity the initial conditions of the flowmeters were set such that  $F_1$  (direct nitrogen) and  $F_2$  (water vapour) were fully closed (0.0 L/min) for 2 min, i.e. the baseline humidity inside the chamber was recorded. Measurements were then repeated with  $F_1$  fully open (1.0 L/min) whilst  $F_2$  was kept fully closed (0.0 L/min) until the signal stabilised (approximately 3.5min). Then,  $F_1$  was reduced by 20% and  $F_2$  was increased to 20% of full scale ( $F_1 = 0.8$  L/min,  $F_2 = 0.2$  L/min) until there was no change in the signal (~3.5min). The flowmeter values were then changed in intervals of 20% until  $F_1$  was fully closed and  $F_2$  was fully open.

The Petri dish acts as a measurement chamber containing the POFHS connected to the tungsten halogen light source at one end and to the spectrometer at the other end to obtain continuous measurement of the transmission spectrum as the RH was varied. In order to provide a reference

standard, a commercial humidity sensor (iButton Hygrochron Temperature/Humidity Logger, DS1923, 0 to 100%RH, Maxim Integrated Ltd.) was also located inside the chamber.

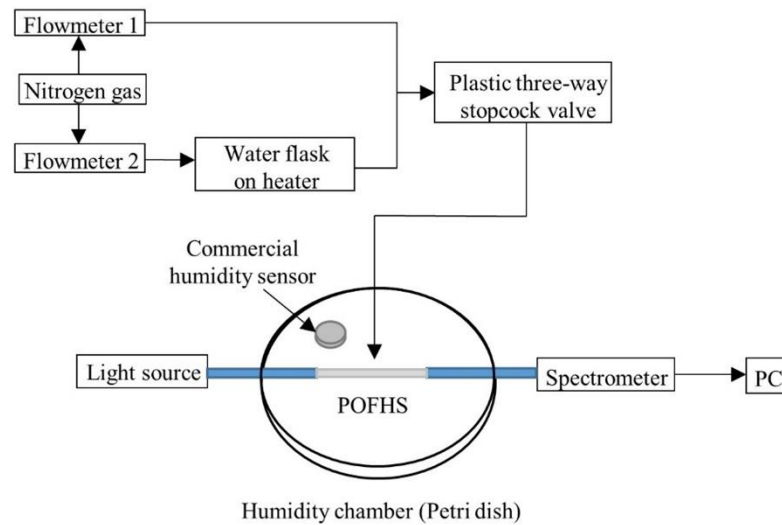


**Figure 3.** In-vitro humidity experiment with flowmeters and POFHS located inside a petri dish which acts as a humidity chamber.

### 2.3 *In-vitro humidity measurement using environmental chamber*

A series of three test were performed using an environmental chamber (Bench Top, C-TH40-20/1, CVMS °Climatic Ltd., UK) to control RH and temperature conditions. The characteristics of the environmental chamber are: 40L internal capacity with dimensions of 300mm x 400mm x 300mm, depth, height and width, respectively. Temperature range of -20°C to 150°C and humidity range of 30% to 98%  $\pm 2.5\%$  RH. The environmental chamber flows cold and hot air to change temperature and a compressor, a condenser and an evaporator are used for changing RH within the chamber. The control of temperature and RH is made by a programmable logic controller (PLC, TEMI 1500).

In the experimental setup, as shown in Figure 4, the POFHS is inserted in the centre of the environmental chamber through portholes (50mm diameter) on each side of the chamber. The tungsten halogen light source and the spectrometer are connected to each end of the POFHS to obtain measurements and compare the data obtained with the environmental chamber sensor.

The first test consisted in varying RH from 90% to 97% and vice versa with fixed temperature at 30°C. In the second test, temperature was changed along the time from ~25°C to 35°C and vice versa with RH constant at 90%. The third test consisted on setting RH and temperature constant for a long period at 85% and 30°C, respectively, to observe the response, repeatability and stability of the POFHS.

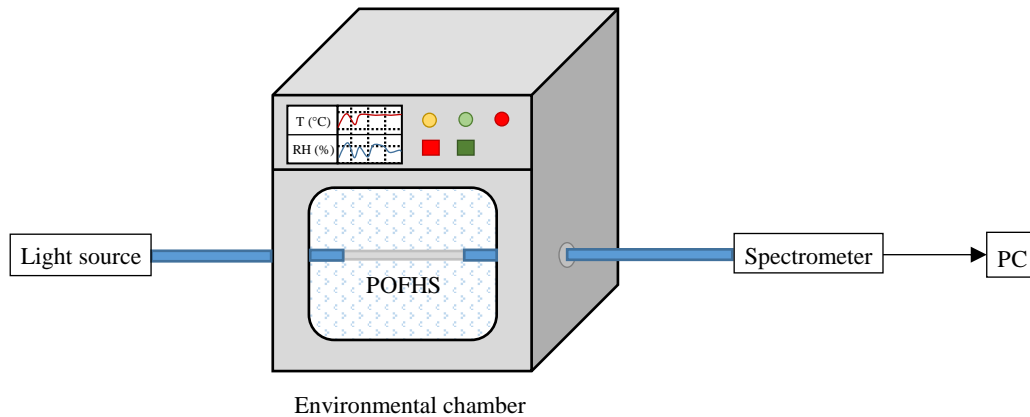


**Figure 4.** Experimental setup for humidity and temperature test with POFHS within environmental chamber.

#### 2.4 *In-vivo humidity measurement*

For the in-vivo humidity test on skin, a similar optical set-up as the above in-vitro test was deployed (Figure 5). The POFHS was inserted inside the measurement chamber along with the reference standard device. On this occasion the sealed lid of the chamber and the flowmeters were replaced by the palm of a human hand. The in-vivo test involved covering the chamber with the palm of the subject's hand until the output signal from the spectrometer stabilised and then removing the hand until the output signal stabilised. This process was repeated 3 times so as to ascertain repeatability of measurements. The experiment was carried out at room temperature (23°C) with measurements on 5 different volunteers (male, healthy, age 25 – 35) recorded. Before the test, all volunteers cleaned their hands with a commercial antibacterial and alcohol-free hand foam sanitiser (Ecohydra) in order to stabilise the skin to the same condition for each participant. Ethical approval was provided by the Ethics Committee, Faculty of Engineering, University of Nottingham.



Change in humidity levels in the in-vitro experiments was limited by the flowmeters and in the case of in-vivo measurements by the release of water vapour from the skin. An additional experiment was therefore conducted to investigate the response time of the POFHS and the commercial humidity sensors by applying short rapid breaths to the measurement chamber.

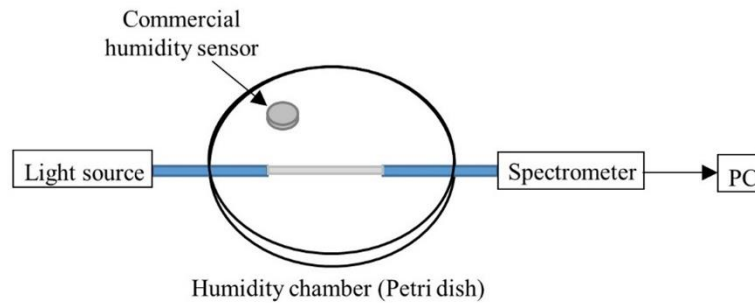


**Figure 5.** Set up for in-vivo humidity test on human skin using the POFHS.

### 3. Results

#### 3.1 Sensor fabrication monitoring

The optimum core diameter for film deposition was  $190 \pm 5 \mu\text{m}$  which can be reached after 27 minutes immersion in acetone since at this diameter a complete removal of cladding and a more uniform surface can be achieved, compared with  $210 \mu\text{m}$  core diameter as shown in the SEM images taken from the unclad section of the fibre (Figure 6). Further etching time produced a fragile fibre and hence will not be practical for applications in wound dressings. At a core diameter of  $190 \mu\text{m}$  different sensing region lengths (5, 10, 20 and 30mm) were also investigated.

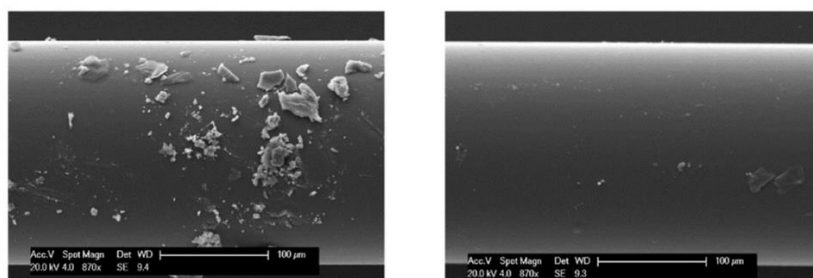


**Figure 6.** SEM image of a  $210 \mu\text{m}$  core diameter POF (left) and a  $190 \mu\text{m}$  core diameter POF (right). Scale bar =  $100 \mu\text{m}$  in both images.

In order to compare the interaction of the evanescent wave with different lengths of sensitive region, the peak intensity of the spectra at wavelength 611nm was measured. Figure 7 illustrates the transmittance at  $\lambda = 611\text{nm}$  as a function of the sensitive region length for four fibres with  $190\mu\text{m}$  core diameter. It was observed that with an increased length of cladding removed, less light intensity was transmitted to the spectrometer. This was expected since more light is able to escape from the unclad section of the fibre, which also increases the EW region that interacts with the hydrophilic film and the surrounding environment. Nonetheless, longer exposed regions produced a fragile fibre and therefore was not practical for applications in wound dressings. The standard deviation is less than 1%, therefore error bars are not plotted on the graph.

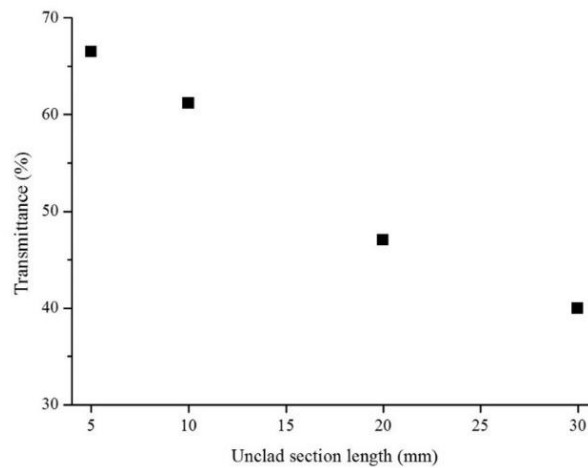


**Figure 7.** Comparison of transmittance at 611nm wavelength versus length of the unclad section of the POF after cladding removal. Core diameter =  $190\mu\text{m}$ .

The optimum length in terms of mechanical robustness and sensitivity of the sensitive region for the POF was 30mm and  $190\mu\text{m}$  core diameter. Figure 8 illustrates the increment in transmittance versus wavelength as more layers are added to the fibre for the whole spectra (Figure 8a) and at 611nm wavelength (Figure 8b). After depositing the 7<sup>th</sup> layer, it can be seen that only a small change in intensity occurs. This can be explained with reference to the relationship between EW penetration depth and film thickness. Optimum film thickness needs to be lower than or equal to the EW penetration depth as sensitivity decreases due to the lack of interaction between EW and the surrounding environment [16].

In this case, the POFHS has a refractive index of 1.49 and 1.22 for the core and the hydrophilic film [25], respectively. For measurements at the wavelength peak of 611nm and angle of incidence  $57^\circ$ , the penetration depth of the EW is approximately 360nm. Since a PAH/SiO<sub>2</sub> layer is approximately 45nm thick, after 7 layers are deposited the film thickness is close to the EW penetration depth.

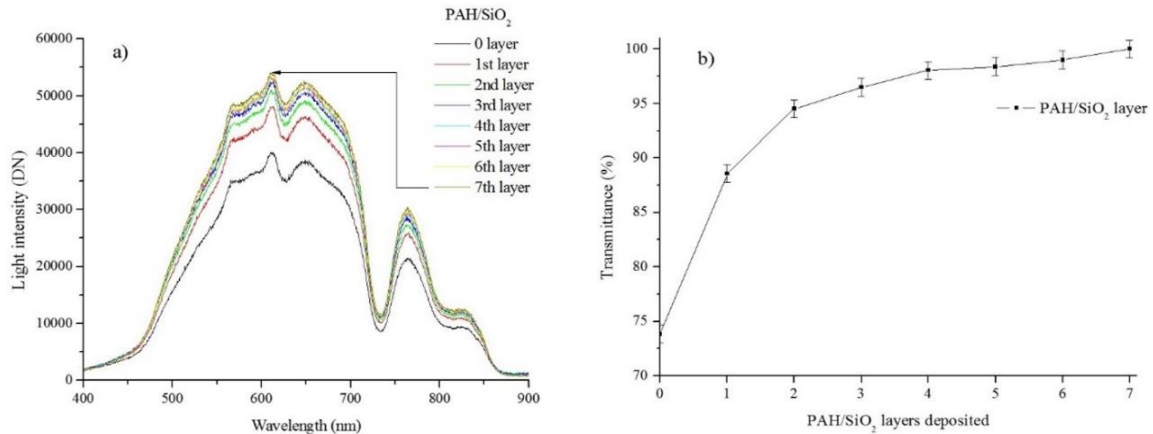


**Figure 8.** (a) POFHS light spectra along film deposition which illustrates that as more layers are deposited, light intensity increases. (b) Transmittance at 611nm wavelength versus number of layers deposited. After the 7<sup>th</sup> layer the sensitivity starts to decrease due to the relationship between film thickness and EW penetration depth.

### 3.2 *In-vitro* humidity measurement based on flowmeter setup

The intensity at the 611nm wavelength peak is illustrated in Figure 9 for a fibre with 190 $\mu$ m core diameter and 7 PAH/SiO<sub>2</sub> layers deposited on a 30mm sensitive region (red trace) compared to the capacitive humidity sensor (blue trace). As can be seen, the POFHS can clearly detect humidity changes and also has a faster response time compared with the capacitive humidity sensor as the RH was changed. The sensor settling time is defined as the time at which the light intensity stabilises within 2% of the maximum value recorded for humidity level. The average settling time for the POFHS was 23s whereas for the commercial sensor the average settling time was 45s. It should be noted that this is not representative of the response time of the POFHS as the change in the humidity in the chamber is gradual.

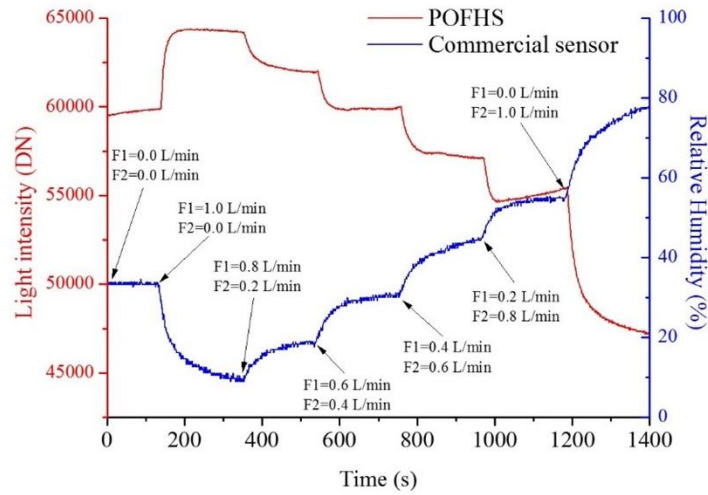


**Figure 9.** In-vitro humidity measurement with flowmeters  $F_1$  and  $F_2$  gradually adjusted in steps of 20% to vary humidity in the chamber. All results were monitored at 611nm wavelength for the POFHS with 7 PAH/SiO<sub>2</sub> layers deposited.

Figure 10 shows the calibration curves for in-vitro humidity measurements with POFHS coated with 5 and 7 PAH/SiO<sub>2</sub> layers. Measurements were taken at 611nm wavelength for both sensors (190 $\mu$ m core diameter and 30mm sensitive region length). It can be observed that the POFHS sensitivity increases as the number of layers increases. After 7 PAH/SiO<sub>2</sub> layers are deposited, the POFHS demonstrated a sensitivity of  $-3.87 \times 10^{-3}$  in transmittance percentage per RH percentage for the range of  $\sim 10\%$  to  $\sim 75\%$  RH. The thickness of 7 PAH/SiO<sub>2</sub> layers is the closest to the EW penetration depth and provides optimal performance, since higher interaction of EW and the hydrophilic film can be achieved.

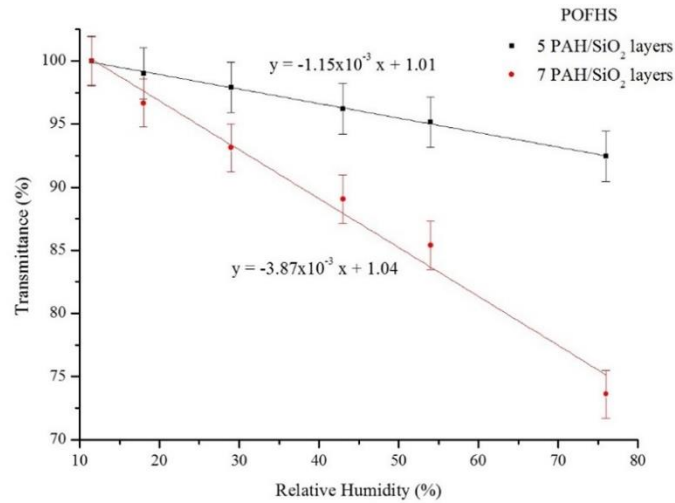


**Figure 10.** In-vitro calibration curves of a POFHS coated with 5 and 7 PAH/SiO<sub>2</sub> layers. Measurements were taken at 611nm wavelength, 190μm core diameter and 30mm sensitive region length for both sensors.

### 3.3 *In-vitro* humidity measurement based on environmental chamber

Figure 11a shows the results for the first test performed with the environmental chamber setup where RH was changed from 90% to 97% and vice versa every 30 minutes. The temperature was set constant at 30°C (Figure 11b). It can be noted that the POFHS response (red trace) is following perfectly the humidity change measured using the environmental chamber sensor (blue trace). Repeatability can be observed in the measurements recorded at 611nm wavelength for the POFHS with 7 PAH/SiO<sub>2</sub> layers, Figure 11a. The linearity observed shows a sensitivity of  $-9.61 \times 10^{-3}$  in transmittance percentage per RH percentage in the range of 90% to 97% RH, Figure 12.

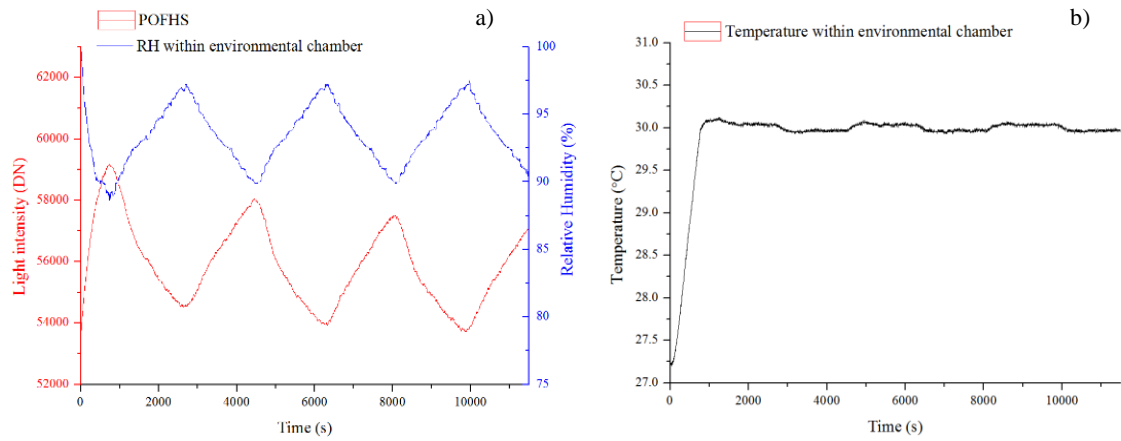


**Figure 11.** First test with POFHS with 7 PAH/SiO<sub>2</sub> layers within environmental chamber setup. (a) POFHS (red trace) and environmental chamber sensor (blue trace) response to humidity in the range of 90% to 97% RH. (b) Temperature recorded during the test, set at 30°C.

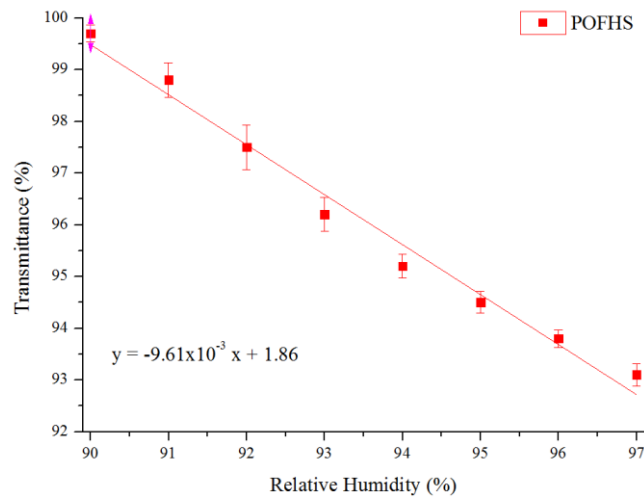


**Figure 12.** Calibration curve of POFHS coated with 7 PAH/SiO<sub>2</sub> layers. Measurements were taken at 611nm wavelength, 190μm core diameter and 30mm sensitive region length. RH range from 90% to 97%.

The second test consists of cycling the temperature from ~25°C to 35°C while trying to maintain RH at 90% using the environmental chamber. Since temperature and RH are related, it can be seen that RH fluctuates (Figure 13a) as temperature was changed from ~25°C to 35°C (Figure 13b) and backwards. Nevertheless, the POFHS behaviour is proportional to that recorded by the environmental chamber sensor (Figure 13a) which indicates that the sensor is

sensitive to the RH rather than to the temperature. It should be also noted that RH sensor in environmental chamber saturates at 100% (blue trace, Figure 13a) and cuts the top off the readings, while the POFHS continuously measures the change in RH. The behaviour of the environmental chamber RH sensor is most likely due to the error of the accuracy of the RH sensor which is quoted as  $\pm 2.5\%$  and measurement range of up to 98%.

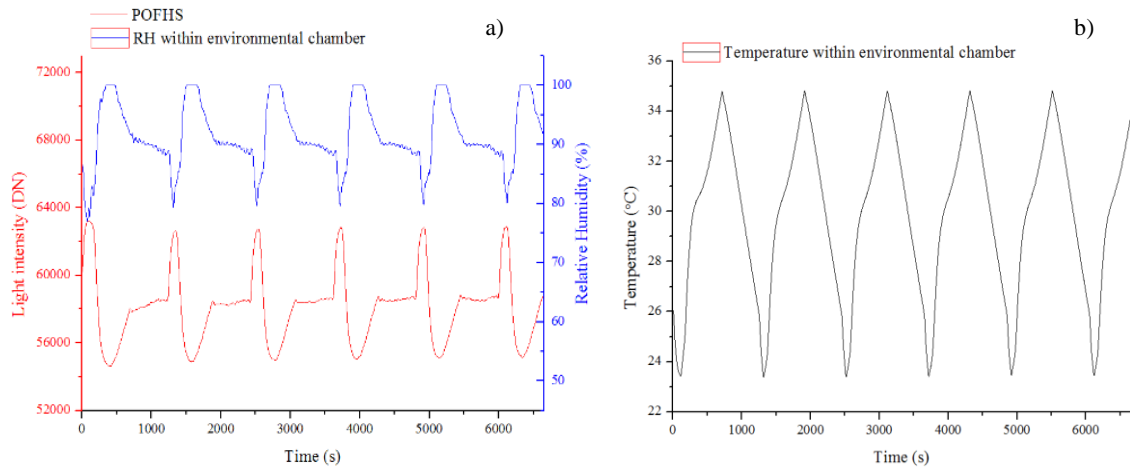


**Figure 13.** Second test with POFHS with 7 PAH/SiO<sub>2</sub> layers within environmental chamber setup. (a) POFHS (red trace) and environmental chamber sensor (blue trace) response to RH fluctuation for temperature changes. (b) Temperature change from  $\sim 25^{\circ}\text{C}$  to  $35^{\circ}\text{C}$  and vice versa.

In the third test, the POFHS response was measured for a long period with constant RH and temperature at 85% and  $30^{\circ}\text{C}$ , respectively. As can be seen in Figure 14a, the POFHS response is stable compared with the environmental chamber sensor. Using the calibration curve (Figure 12), the POFHS signal can be expressed in terms of RH, Figure 14b. It can be noticed that the POFHS response is reliable for long term measurements, therefore it can be used for continuously monitoring wound healing.

In addition, in order to understand behaviour of the plastic optical fibre, an optical fibre with cladding removed ( $190\mu\text{m}$  core diameter) without coating was inserted within the setup during the long period test. As can be seen in Figure 14a, the response of the unmodified fibre (black trace) is not stable at fixed values of RH compared with the POFHS signal. This phenomenon most plausibly is owing to the swelling of the plastic optical fibre. On the other hand, POFHS

(i.e. modified with the sensitive film 7 PAH/SiO<sub>2</sub> layers) has stable response, most likely owing to the protection role that 7 PAH/SiO<sub>2</sub> layers play and adsorb water molecules preventing them from absorption inside the plastic optical fibre.

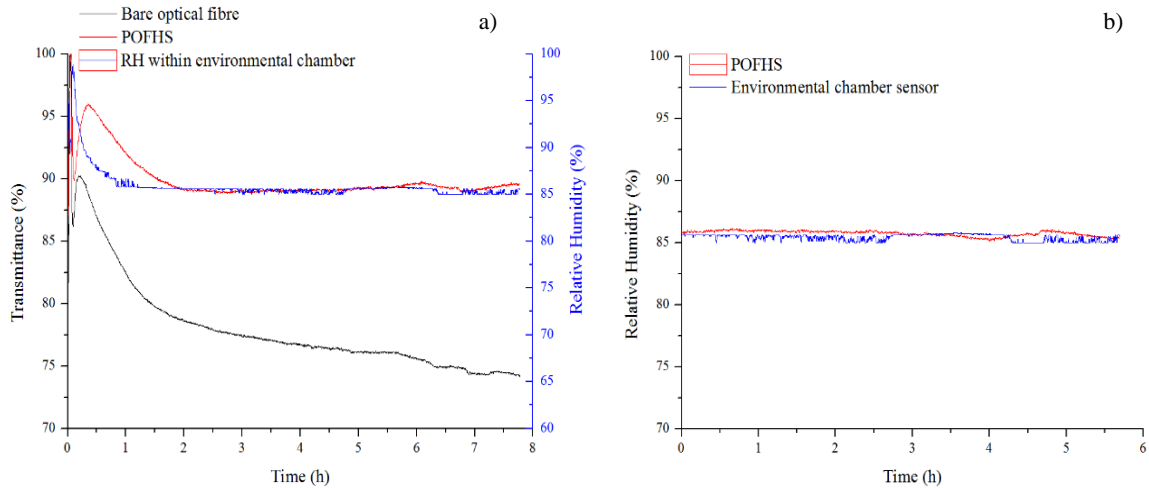


**Figure 14.** Third test with environmental chamber setup. (a) Response from POFHS (red trace), environmental chamber sensor (blue trace) and optical fibre without film and core exposed (black trace) to continuous RH measurement. Temperature and RH constant at 30°C and 90%, respectively for approximately 8hrs. (b) POFHS readings (red trace) in terms of RH compared with environmental chamber sensor (blue trace).

### 3.4 *In-vivo humidity measurements*

The purpose of the in-vivo humidity test was to monitor the RH present on the skin microenvironment at the palm of the hand to mimic the wound environment. As described in section 3.2, the study consisted of placing the palm on the measurement chamber as shown in Figure 5 and monitoring transmittance in order to observe the RH changes within the chamber. The hand was removed from the top of the chamber after the signal stabilised.

Figure 15 shows the results for the in-vivo humidity measurements on skin for one of the participants at 611nm wavelength since similar results were obtained with all the volunteers. Using the calibration curve (Figure 10), the signal obtained from the POFHS can be observed in terms of RH in order to measure the response time compared with the commercial sensor.



The variation of RH recorded for each participant was from  $50 \pm 5\%$  to  $90 \pm 5\%$ . When removing the hand from the chamber, a rapid drop in RH occurs due to the difference between the RH inside the measurement chamber and the environment. This sudden RH change is observed in both the POFHS and the commercial humidity sensor signals. The hand was placed again on the chamber after the signal stabilised again. This operation was repeated 3 times in order to investigate repeatability of the measurements for each volunteer. The settling time, which is the time for the signal to reach 90% of saturated value was  $100 \pm 3\text{s}$  and  $135 \pm 3\text{s}$ , for the POFHS and the commercial sensor, respectively. As expected, the same behaviour as for the in-vitro humidity measurements was observed, i.e. an increase in RH represents a decrease in light intensity. Again, these response times are limited by the rate of increase of humidity in the chamber and not the response time of the sensors.

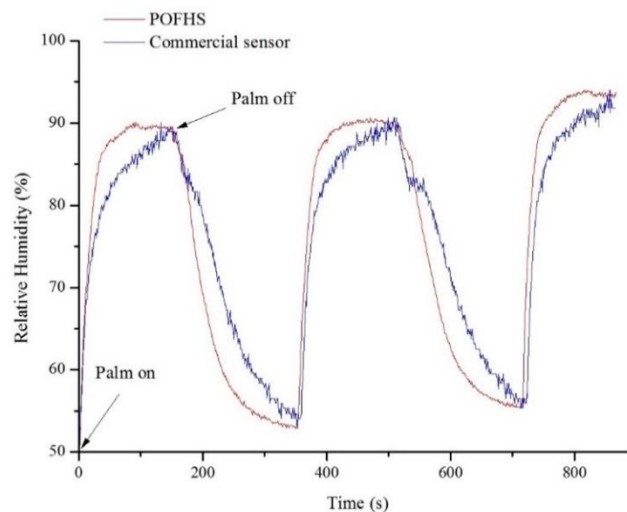


**Figure 15.** In-vivo humidity measurements on the palm of the hand recorded with the POFHS (red trace) and the commercial humidity sensor (blue trace).

In order to further investigate the POFHS response time, a more rapid change in humidity is provided using a sharp breath on the sensor. Figure 16 displays relative humidity measured at 611nm wavelength for the POFHS (red trace) along with the commercial humidity sensor response (blue trace) in RH. The response time is calculated as the time from 10% to 90% of the final recorded value. The POFHS response time recorded was 1.5s, whereas the value observed with the commercial sensor was 3.1s.

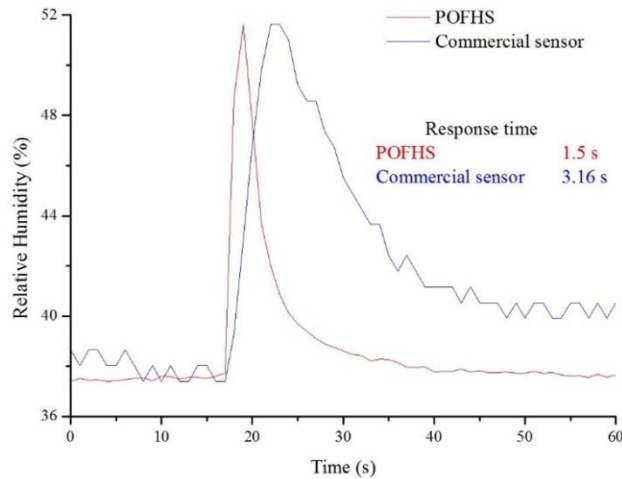


**Figure 16.** Response time of POHFS and commercial humidity sensor in response to a single breath on both sensors simultaneously.

#### 4. Discussion

The development of a POHFS is reported. Different lengths and core diameter for the sensitive part of the fibre were investigated. The optimum core diameter and length of the sensitive region were 190 $\mu$ m and 30mm, respectively, in order to obtain higher sensitivity due to deeper penetration depth of EW and interaction with the hydrophilic film coated on the unclad central section of a POF. Smaller core diameters and longer sensitive regions produce a fragile sensor which tends to easily break.

The physical behaviour of the POHFS against RH changes is related to the film refractive index. When the sensor is exposed to dry environments, the core refractive index is higher than the PAH/SiO<sub>2</sub> coating refractive index. As a result, the fibre works as a wave-guide and hence transmittance of light increases. On the other hand, when the sensor is exposed to humid surroundings, the refractive index of the sensitive PAH/SiO<sub>2</sub> section increases until it is higher than that of the core, hence the light scatters through the film and the transmittance is reduced.

Additionally, the humidity in-vitro measurements were carried out at different RH and temperature conditions. The POHFS response was proportional to the RH and temperature

changes. For the humidity test on the palm of the hand, temperature and ambient light did not affect measurements since both parameters were not significantly changing when placing the hand on the set up.

In order to achieve a portable set up for practical applications, such as the performance of the POFHS within a dressing, a photodetector can replace the spectrometer function of collecting the data from the sensor. The light source that can be also exchanged for an LED in order to reduce the set up size. This is useful for tele monitoring purposes and to obtain a low-cost portable device.

Furthermore, as a first step for wound monitoring development, the POFHS has been embedded on a dressing (sterile, N-A knitted viscose primary dressing, Systagenix Wound Management Ltd., UK) with dimensions 9.5cm length and 9.5cm width and it was covered by a clinical gauze used as secondary dressing (non-woven swab clinic gauze, Clinisupplies Ltd., UK) with dimensions 5cm length and 5cm width in order to observe its feasibility for humidity measurements, as shown in Figure 17a. In order to observe the POFHS response embedded on the dressing, the in-vivo humidity experiment was performed for a single volunteer.

Figure 17b shows the response of the POFHS to the RH generated by the palm of the hand. As it can be seen on the graph, the behaviour of the POFHS is similar to the previous in-vivo test in section 3.4. Nonetheless, since the POFHS is embedded on the dressing and it is covered by a clinical gauze, a longer settling time is observed. It should be noted that the response is highly dependent on the properties of the textile and further work investigating responses of different wound dressings will form part of future work.

The settling time and the recovery time obtained were  $\sim 7.7$  min and  $\sim 9.7$  min, respectively. The RH change observed was between  $30\% \pm 2\%$  and  $95\% \pm 2\%$ . This are encouraging results in order to develop a dressing that can remotely monitor humidity in the skin microenvironment and that can be helpful to provide better prognosis of wound healing.

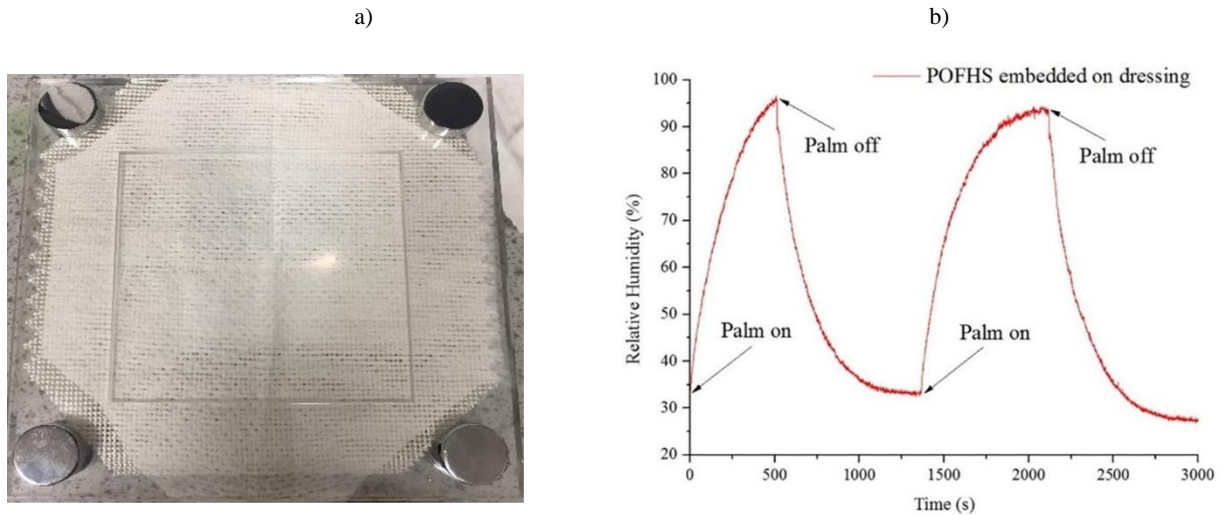


**Figure 17.** (a) POFHS embedded in a dressing and covered by a clinical gauze as a secondary dressing for humidity measurements. The unclad visible part of the sensor is 30mm length. (b) In-vivo humidity measurements on the palm of the hand recorded with the POFHS embedded on a dressing and covered with a clinical gauze as secondary dressing.

Moreover, in future generations of the device, the sensor might be incorporated into a smart wound dressing that can control the temperature and humidity of the wound microenvironment. For example, the device could take a similar form to a vacuum assisted closure (VAC) system, in which a feedback loop is created to control humidity levels [26].

## 5. Conclusion

In this work, it has been demonstrated that a POF coated with PAH/SiO<sub>2</sub> layers on the exposed core can be used as a humidity sensor. A higher RH sensitivity can be obtained by optimising the film thickness depositing 7 PAH/SiO<sub>2</sub> layers which is close to but lower than the EW penetration depth. The sensitivity demonstrated for 7 layers deposited was  $-3.87 \times 10^{-3}$  and  $-9.61 \times 10^{-3}$  in transmittance percentage per RH percentage for the range of ~10% to ~75% RH and 90% to 97% RH, respectively.

The deposition of SiO<sub>2</sub> nanoparticles as a sensitive element has provided pilot data to illustrate its efficiency in the detection of humidity. The RH measurements in the in-vivo tests suggest

that the POFHS developed can be used as a humidity sensor of the human skin. The POFHS response time is in the order of 1.5s compared to the commercial humidity sensor of 3.1s, for breath monitoring (rapid RH changes). In addition, for measurements on skin, the POFHS average settling time observed was 1.6 min, faster than settling time recorded by the commercial sensor (approximately 2.6 min). Further, the POFHS feasibility to be integrated within a dressing was tested by embedding the POFHS into a textile. The results obtained suggests that a POFHS within a dressing can be developed in order to monitor moisture in wounds.

The development of POFHS is a novel technology that provides a faster response, compared with a commercial humidity sensor. The POFHS advantages are flexibility, ease of incorporation into dressings and immunity to electromagnetic fields. This new and reliable unobtrusive approach for humidity sensing is potentially extremely helpful for providing improved monitoring of wound status. If successful it will be of increased benefit for patients and offers the potential to allow a better understanding about the process of wound healing itself.

### **Acknowledgements**

Funding was obtained from the Engineering and Physical Sciences Research Council (grant number EP/K503800/1). David Gomez was funded by the National Council on Science and Technology of Mexico (CONACYT). We would also like to thank Prof William Jeffcoate and Alison Musgrove of Nottingham University Hospitals NHS Trust for valuable clinical discussions.

### **References**

- [1] F. U. Hernandez, S. P. Morgan, B. R. Hayes-Gill, D. Harvey, W. Kinnear, A. Norris, D. Evans, J. G. Hardman and S. Korposh, "Characterization and Use of a Fiber Optic Sensor Based on PAH/SiO<sub>2</sub> Film for Humidity Sensing in Ventilator Care Equipment," *IEEE Transactions on Biomedical Engineering*, vol. 63, no. 9, pp. 1985-1992, 2016.

- [2] G. D. Winter, "Formation of the Scab and the Rate of Epithelialization of Superficial Wounds in the Skin of the Young Domestic Pig," *Nature*, vol. 193, pp. 293-294, 1962.
- [3] J. F. Guest, N. Ayoub, T. Mc Ilwraith, I. Uchegbu, A. Gerrish, D. Weidlich, K. Vowden and P. Vowden, "Health economic burden that wounds impose on the National Health Service in the UK," *BMJ Open*, vol. 5, no. 12, pp. 1-8, 2015.
- [4] L. G. Ovington, "Advances in wound dressings," *Clinics in dermatology*, vol. 25, pp. 33-38, 2007.
- [5] K. Cutting, R. White, P. Mahoney and K. Harding, *Clinical identification of wound infection: a Delphi approach*, London: European Wound Management Association (EWMA) Position Document, 2005.
- [6] G. S. Schultz, R. G. Sibbald, V. Falanga, E. A. Ayello, C. Dowsett, K. Harding, M. Romanelli, M. C. Stacey, L. Teot and W. Vanscheidt, "Wound Bed Preparation: A Systematic Approach to Wound Management," *Wound Repair And Regeneration, The International Journal of Tissue Repair and Regeneration*, vol. 11, pp. 1-28, 2003.
- [7] M. Dyson, S. Young, C. L. Pendle, D. F. Webster and S. M. Lang, "Comparison of the Effects of Moist and Dry Conditions on Dermal Repair," *The Journal of Investigative Dermatology*, vol. 91, pp. 434-439, 1988.
- [8] T. Abdelrahman and H. Newton, "Wound dressings: principles and practice," *Surgery*, vol. 29, no. 10, pp. 491-495, 2011.
- [9] M. A. Fonder, G. S. Lazarus, D. A. Cowan, B. Aronson-Cook, A. R. Kohli and A. J. Mamelak, "Treating the chronic wound: A practical approach to the care of nonhealing wounds and wound care dressings," *Journal of the American Academy of Dermatology*, vol. 58, no. 2, pp. 185-206, 2008.
- [10] K. F. Cutting and R. J. White, "Maceration of the skin and wound bed 1: its nature and causes," *Journal of wound care*, vol. 11, no. 7, pp. 275 - 278, 2002.
- [11] T. Yeo, T. Sun and K. Grattan, "Fibre-optic sensor technologies for humidity and moisture measurement," *Sensors and Actuators A: Physical*, vol. 144, no. 2, pp. 280-295, 2008.

- [12] S. D. Milne, P. Connolly, H. Al Hamad and I. Seoudi, "Development of Wearable Sensors for Tailored Patient Wound Care," in *Engineering in Medicine and Biology Society (EMBC), 2014 36th Annual International Conference of the IEEE*, 2014.
- [13] G. Mattana, T. Kinkeldei, D. Leuenberger, C. Ataman, J. J. Ruan, F. Molina-Lopez, A. Vásquez Quintero, G. Nisato, G. Tröster, D. Briand and N. F. de Rooij, "Woven Temperature and Humidity Sensors on Flexible Plastic Substrates for E-Textile Applications," *IEEE Sensors Journal*, vol. 13, no. 10, pp. 3901-3909, 2013.
- [14] R. Soukup, A. Hamacek, L. Mracek and J. Reboun, "Textile Based Temperature and Humidity Sensor Elements for Healthcare Applications," in *37th International Spring Seminar on Electronics Technology (ISSE)*, Dresden, Germany, 2014.
- [15] D. Gomez, S. P. Morgan, B. R. Hayes-Gill and S. Korposh, "Polymeric fibre optic sensor based on a SiO<sub>2</sub> nanoparticle film for humidity sensing on wounds," in *Sixth European Workshop on Optical Fibre Sensors*, Limerick, Ireland, 2016.
- [16] S. K. Khijwania, K. L. Srinivasan and J. P. Singh, "An evanescent-wave optical fiber relative humidity sensor with enhanced sensitivity," *Sensors and Actuators B: Chemical*, vol. 104, no. 2, pp. 217-222, 2005.
- [17] F. S. Ligler and C. Rower Taitt, *Optical Biosensors: Today and Tomorrow*, Oxford: Elsevier, 2008.
- [18] B. D. Gupta and Ratnanjali, "A novel probe for fiber optic humidity sensor," *Sensors and Actuators B: Chemical*, vol. 80, pp. 132-135, 2001.
- [19] L. Xu, J. C. Fanguy, K. Soni and S. Tao, "Optical fiber humidity sensor based on evanescent-wave scattering," *Optics Letters*, vol. 29, no. 11, pp. 1191-1193, 2004.
- [20] K. S. C. Kuang, S. T. Quek, C. G. Koh, W. J. Cantwell and P. J. Scully, "Plastic Optical Fibre Sensors for Structural Health Monitoring: A review of recent progress," *Journal of Sensors*, vol. 2009, pp. 1-13, 2009.
- [21] S. Korposh, T. Wang, S. James, R. Tatam and S.-W. Lee, "Pronounced Aromatic Carboxylic Acid Detection Using a Layer-By-Layer Mesoporous Coating on Optical

Fibre Long Period Grating,” *Sensors and Actuators B: Chemical*, vol. 173, pp. 300-309, 2012.

- [22] T. R. Dargaville, B. L. Farrugia, J. A. Broadbent, S. Pace, Z. Upton and N. H. Voelcker, “Sensors and Imaging for Wound Healing: A Review,” *Biosensors and Bioelectronics*, vol. 41, pp. 30-42, 2013.
- [23] D. Viegas, J. Goicoechea, J. L. Santos, F. Moita Araujo, L. A. Ferreira, F. J. Arregui and I. R. Matias, “Sensitivity Improvement of a Humidity Sensor Based on Silica Nanospheres on a Long-Period Fiber Grating,” *Sensors*, vol. 9, pp. 519 - 527, 2009.
- [24] S. Korposh, S. James, R. Tatam and S.-W. Lee, “Fibre-Optic Chemical Sensor Approaches Based on Nanoassembled Thin Films: A Challenge to Future Sensor Technology,” *Current Developments in Optical Fiber Technology*, pp. 237-264, 2013.
- [25] J. Bravo, L. Zhai, Z. Wu, R. E. Cohen and M. F. Rubner, “Transparent Superhydrophobic Films Based on Silica Nanoparticles,” *Langmuir*, vol. 23, no. 13, pp. 7293-7298, 2007.
- [26] K. V. Lambert, P. Hayes and M. McCarthy, “Vacuum Assisted Closure: A review of development and current applications,” *European Journal of Vascular and Endovascular Surgery*, vol. 29, no. 3, pp. 219-226, 2005.